

## Formation of $Y_2O_3$ nanodots on substrate surface using the rf-sputtering method

K. C. Chung<sup>1,\*</sup>, J. M. Yoo<sup>1</sup>, Y. K. Kim<sup>1</sup>, X. L. Wang<sup>2</sup>, S. X. Dou<sup>2</sup>

<sup>1</sup>Korea Institute of Materials Science, 66 Sangnam-dong, Changwon 641-010, Korea

<sup>2</sup>Institute for Superconducting and Electronic materials, Univ. of Wollongong, Wollongong NSW2522, Australia

**Abstract--**  $Y_2O_3$  nanodots have been deposited on top of the substrate surface using rf-sputtering method. This approach was adopted to be able to modulate the substrate surface with nanodots used as a seed for the flux pinning sites in the superconducting films. The nanodot density of  $Y_2O_3$  was controlled mainly using the deposition time, rf-power, and substrate temperature.  $Y_2O_3$  nanodots with  $\sim 50$  nm in diameter and  $\sim 3$  nm in height were obtained at rf-sputtering time of about 15 seconds using 400 watts of rf-power and  $630^\circ\text{C}$  of substrate temperature. As deposition time increased up to about 30 seconds, the interconnected islands of  $Y_2O_3$  nanodots formed, which can be clearly observed with AFM surface image. The substrate surface was covered entirely with  $Y_2O_3$  layer above the deposition time of 60 seconds. The modulated surface morphologies and cross section analysis of deposited  $Y_2O_3$  nanodots at various experimental conditions have been examined using AFM and discussed with respect to the flux pinning sites for the practical application.

### 1. INTRODUCTION

For the potential applications of high  $T_c$  superconducting coated conductors such as commercial motors, generators, and military uses, the large critical currents in applied magnetic fields are highly required [1]. The performance requirements for these applications are such that the flux pinning sites like dislocations, oxygen vacancies, and stacking faults that are defects naturally existed in superconducting materials cannot meet due to their rather lower density [1, 2]. Thus, introducing the artificial pinning sites for enhanced current carrying performance in high magnetic fields have been necessarily considered and studied extensively [1-4]. Among the artificial pinning sites, columnar defects introduced by heavy ion irradiation and comprised of self-assembled nanodots were well known to be especially strong to pin the magnetic flux lines applied parallel to them [1,3]. Moreover, the obtained in-field  $J_c$  in applied magnetic fields showed very promising results to be used in practical applications. However, these methods are very expensive and limited to be applicable to large scale and long length fabrication of superconducting coated conductors.

Here, we propose our strategy to induce the columnar defects, which have been known as one of the strongest flux pinning sites in high  $T_c$  superconducting materials [1,

3]. To induce the columnar defects in superconducting materials deposited on substrate, the surface of substrate need to be modulated with the formation of nanodots dispersed uniformly on it. Because the deposited superconducting phase on top of the nanodots cannot form due to the misfit strain of lattice mismatch between the two layers and chemical poisoning, the columnar defects can be induced on top of the nanodots as a seed [4].

Also, it is highly desirable to prepare the surface-modulated templates consisted of buffered metal substrates and nanodots on it using the single deposition method such as a sputtering, which are industrially scalable and cost effective[5,6].

In this work, rf-sputtering method was adopted to form the nanodots on the surface of substrates [4,7]. The formation of nanodots was investigated using the atomic force microscopy (AFM). The size and density of nanodots were examined and discussed for the effective flux pinning sites in superconducting materials.

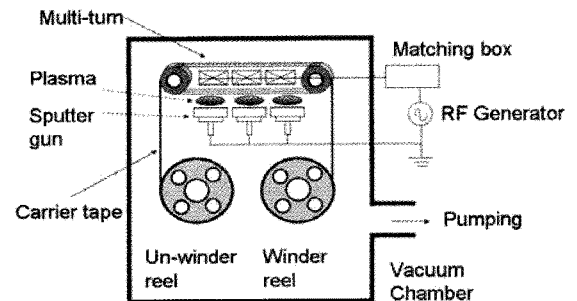


Fig. 1. Schematic view of multi-turn reel-to-reel rf-sputtering system for nanodot formation.

### 2. EXPERIMENTAL

$Y_2O_3$  has been deposited using rf-sputtering method as shown in Fig. 1. The base pressure of the rf-sputtering system reached to the  $7 \times 10^{-6}$  Torr using turbo molecular pump and back-up mechanical pump. Then, the chamber was filled with argon gas, which also acted as sputtering gas of  $Y_2O_3$  ceramic target, injected through the sputter was filled

\* Corresponding author: kcchung@kims.re.kr

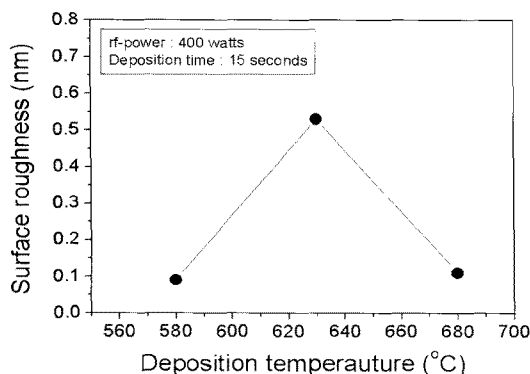


Fig. 2. Surface roughness of  $Y_2O_3$  nanodots measured by AFM. Samples were rf-sputtered at 580, 630, and 680°C respectively. The power of sputtering and deposition time were fixed to 400 watts and 15 seconds for all samples.

with argon gas, which also acted as sputtering gas of  $Y_2O_3$  ceramic target, injected through the sputter gun. The sputtering pressure was controlled using the pendulum valve in the range of 4 to 10 mTorr.  $Y_2O_3$  nanodots were grown on substrates at the deposition temperature of 600 ~ 700°C [4,5]. The rf-sputtering deposition was conducted from 10 seconds to the several minutes. After the rf-sputtering was done for the nanodot formation, the samples were cooled down to room temperature within the same argon ambient.

The surface of substrate,  $LaAlO_3$  (LAO) single crystal, was measured before the  $Y_2O_3$  deposition and identified to have the  $R_a$  (average surface roughness) of less than 0.25 nm. The size and density of  $Y_2O_3$  nanodots were controlled mainly using deposition time, power of rf-sputtering, and substrate temperature [4,7]. The formation of nanodots was studied and analysed by AFM surface image and cross section profile to reveal their size, density, and shape.

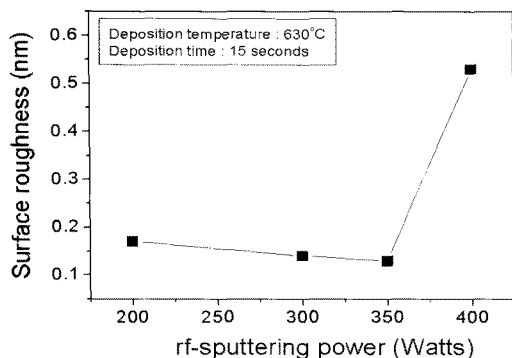


Fig. 3. Surface roughness of  $Y_2O_3$  nanodots measured by AFM. Samples were sputtered at 200, 300, 350, and 400 watts of rf-power. The substrate temperature and deposition time were fixed to 630°C and 15 seconds.

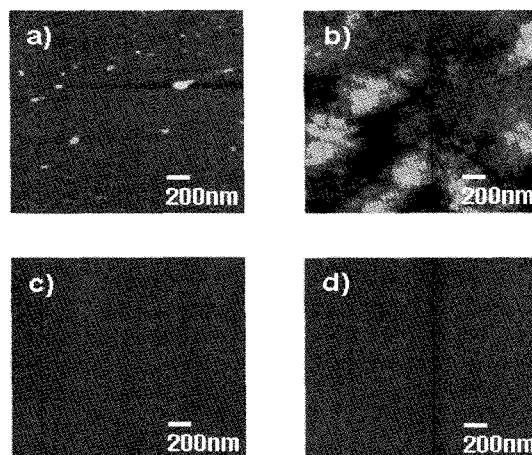


Fig. 4. Surface AFM images of the  $Y_2O_3$  nanodots rf-sputtered at (a) 15, (b) 30, (c) 60, and (d) 180 seconds respectively on LAO single crystal substrates. The deposition was done at 630°C and 400 watts.

### 3. RESULTS AND DISCUSSION

Among the various methods to fabricate the nanodots on top of the substrate surface, rf-sputtering is one of the best candidates. As it is highly possible to prepare the surface-modulated templates consisted of buffered metal substrates and nanodots on it using single deposition method like rf-sputtering, which are low-cost process and can be scaled-up to industrial level for the long length fabrication of superconducting coated conductors[4,5].

First of all, the substrate temperature was changed to investigate the formation of  $Y_2O_3$  nanodots on LAO single crystals. For this experiment, we used 400 watts of rf-power for  $Y_2O_3$  sputtering. This rather high value was actually used for the deposition of  $Y_2O_3$  seed layer on the metal substrate like Ni-5%W tape in our reel-to-reel multi-turn rf-sputtering system. As shown in Fig. 2,  $Y_2O_3$  nanodots were found only at 630°C with surface roughness of 0.52 nm, which increased from the value of ~ 0.25 nm of the bare LAO substrate due to the deposited  $Y_2O_3$  nanodots on the surface.

For the next experiment shown in Fig. 3, we changed the power of rf-sputtering from 400 watts down to 200 watts with deposition time of 15 seconds at 630°C. As described above it is to prevent the possible cracks of sputtering target at high rf-power like around 400 watts. The surface roughness decreased to the ~ 0.13 nm at 350 watts. And there was slight increase of surface roughness as rf-power was lowered further. However, No nanodots are found in AFM images in our experimental condition except the one at 400 watts.

Now, we changed the sputtering deposition time for  $Y_2O_3$  nanodots formation with the other two process variables fixed at 630°C and 400 watts. As can be seen in Fig. 4(a), the roughness of surface with  $Y_2O_3$  nanodots

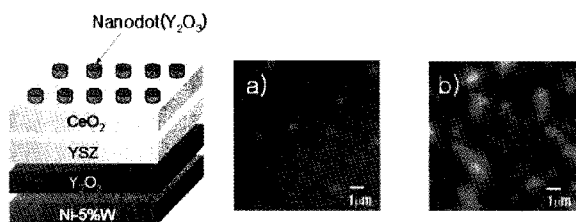


Fig. 5.  $Y_2O_3$  nanodots were formed on the buffered metal substrates as shown on the left using the reel-to-reel multi-turn rf-sputtering system at 400 watts and the moving speed of 40cm/min. (a) AFM surface image of top  $CeO_2$  buffer layer with roughness of 7.7nm and (b) after  $Y_2O_3$  nanodots formation with roughness of 14.4nm.

rf-sputtered at 15 seconds increased to 0.53 nm compared to less than 0.25 nm of the bare LAO substrate. The roughness increased further at 30 seconds to 2.65 nm and the inter-connected islands morphology with irregular shape was observed as in Fig. 4(b). It is obvious that we can obtain the reduced surface roughness of less than 0.14nm above the sputtering time of 1 minute, as the whole surface now can be covered with  $Y_2O_3$  layer shown in Fig. 4 (c, d) respectively.

The size and shape of  $Y_2O_3$  nanodots sputtered on LAO substrates were analyzed using the cross section of AFM images. The typical diameter and height of dots were  $\sim 50$  nm and  $\sim 3$  nm for the sputtering time of 15 seconds with the some bigger dots with  $\sim 100$ nm (Diameter) and  $\sim 30$ nm (Height) in Fig. 4(a). And the calculated number density using the cross section analysis was approximately  $155/\mu m^2$  [1,4,7]. Here, it should be mentioned that the smaller size and the higher number of the density of nanodots will be beneficial for effective flux pinning sites in superconducting materials in applied magnetic fields. In a sense, it will be even advantageous to induce the columnar defects with the height of nanodots comparable to the thickness of superconducting layer.

$Y_2O_3$  nanodots were also rf-sputtered and formed on top of the  $CeO_2$  buffer layer as shown in Fig. 5 for the future application of superconducting coated conductors. The surface roughness of sputtered  $Y_2O_3$  nanodots was 14.4 nm in Fig. 5(b) and this value was about two times than that of top  $CeO_2$  buffer layer, which is about 7.6 nm shown in Fig. 5(a). And the cross section analysis of AFM image revealed that  $Y_2O_3$  nanodots of  $\sim 500$  nm (Diameter) and  $\sim 70$  nm (Height) formed on the buffered metal substrates.

To demonstrate the effectiveness of the nanodots fabricated by rf-sputtering method as a seed on substrate surface for the flux pinning sites in superconducting materials, superconducting layer will be deposited and its flux pinning properties like a  $J_c$  in magnetic fields and microstructure development will be investigated in the future [1,7]. Also, we will study the correlation between the size and shape of nanodots and the flux pinning sites induced inside the superconducting layer.

#### 4. CONCLUSIONS

$Y_2O_3$  nanodots have been grown on the substrate surface using rf-sputtering system, thus enable to modulate surface for the effective pinning sites to be induced inside the superconducting films. Also, it is highly promising to prepare the surface-modulated templates using the single deposition method, which are industrially scalable and cost effective rf-sputtering. The size and distribution of  $Y_2O_3$  nanodots were studied using the AFM surface images and cross section analysis. The density of  $Y_2O_3$  nanodots was about  $155/\mu m^2$  with  $\sim 50$  nm (Diameter) and  $\sim 3$  nm (Height) at deposition time of 15 seconds, deposition temperature of  $630^\circ C$ , and rf-sputtering power of 400 watts.

#### ACKNOWLEDGMENT

This work was supported by the Korea Foundation for International Cooperation of Science & Technology (KICOS) through a grant provided by the Korean Ministry of Education, Science & Technology(MEST) in 2006 (NO. M60602000012).

#### REFERENCES

- [1] S. Kang, A. Goyal, J. Li, A. A. Gapud, P. M. Martin, L. Heatherly, J. R. Thompson, D. K. Christen, F. A. List, M. Paranthaman, D. F. Lee, *Science* 311, pp. 1911, 2006.
- [2] T. Haugan, P. N. Barnes, R. Wheeler, F. Melsenkothen, M. Sumption, *Nature* 430, pp. 867, 2004.
- [3] S. Kang, A. Goyal, J. Li, P. Martin, A. Ijaduola, J. R. Thompson, M. Paranthaman, *Physica C* 457, pp. 41, 2007.
- [4] A. Crisan, S. Fujiwara, J. C. Nie, A. Sundaresan, H. Ihara, *Appl. Phys. Lett* 79, pp. 4547, 2001.
- [5] M. S. Bhuiyan, M. Paranthaman, S. Kang, D. F. Lee, K. Salama, *Physica C* 422, pp. 95, 2005.
- [6] M. Parans Paranthaman, S. Sathyamurthy, L. Heatherly, P. M. Martin, A. Goyal, T. Kodenkandath, X. Li, C. L. H. Thieme, M. W. Rupich, *Physica C* 445-448, pp. 529, 2006.
- [7] A. Pomar, A. Llordés, M. Gibert, S. Ricart, T. Puig, X. Obradors, *Physica C* 460-462, pp. 1401, 2007.